

Applications of non-collinear second harmonic generation in one-dimensional periodically poled crystals

Tal Ellenbogen, Ady Arie *

Department of Physical Electronics, Faculty of Engineering, Tel-Aviv University, Tel-Aviv 69978, Israel

Received 25 March 2007; received in revised form 9 May 2007; accepted 11 May 2007

Abstract

Whereas the commonly used collinear quasi-phase-matched interaction is usually suitable for phase matching only a single nonlinear process, non-collinear interactions offer rich variety of phase matching possibilities, employing different elements of the nonlinear tensor, and various orders of quasi phase matching. By studying the dependence of the second harmonic process on the angle and the phase matching order in a periodically poled LiNbO₃ crystal, we can non-destructively derive the duty cycle of the structure. The obtained duty cycle agrees well with surface scan measurements using an atomic force microscope. Furthermore, by proper selection of the non-collinear angle, we demonstrate simultaneous second harmonic generation of two cross polarized waves.
© 2007 Elsevier B.V. All rights reserved.

Keywords: Frequency conversion; Multiharmonic generation; Nonlinear optics; Devices

Quasi phase matching (QPM) is an efficient method for second harmonic generation (SHG) of a pump wave in a nonlinear crystal [1]. It is common to use collinear interactions, where the pump wave and the second harmonic (SH) wave propagate in the same direction thereby enabling large interaction lengths and efficient conversion. However, non-collinear interactions are much more flexible for applications that require phase matching of more than one process. In this article we demonstrate that non-collinear SHG can be used in one-dimensional periodically poled crystals for characterization of the crystal properties (in particular, the average duty cycle D , defined as the ratio of the length of (say) the positive nonlinear coefficient to the entire period) and for simultaneous generation of cross polarized SH waves. Average duty cycle measurements are very important in order to deduce the phase matching possibilities and efficiencies of different orders of QPM. Simultaneous generation of two states of polarizations cannot be realized

by birefringence and may be used for multi-partite entanglement [2] and for cross polarized wave generation [3].

The efficiency of the nonlinear process in a collinear interaction for the m th QPM order is proportional to $[(2/m\pi) \times \sin(\pi m D)]^2$. It can be calculated from this relation that, for example, the efficiency of a 3rd-order QPM process with a duty cycle of the structure of 67%, is zero. On the other hand, 2nd-order QPM gets its highest efficiency for duty cycles of 25% and 75%, but its efficiency is nullified for duty cycle of 50%. In fact, as the QPM order is increased, the process becomes more sensitive to duty cycle variations. High orders QPM is required, for example, for the generation of short wavelengths, since owing to high dispersion at these wavelengths, the coherence length becomes very small (smaller than the poling resolution). Other processes which require high order QPM are backward generations [4]. For these and similar high order QPM cases it is most desirable to measure the duty cycle which highly affects the efficiency of the process. Duty cycle measurements are also required for electro-optic filtering in PPLN [5], where the performance of the filter is dependent on the duty cycle.

* Corresponding author.

E-mail address: ady@eng.tau.ac.il (A. Arie).

We present here a method to use non-collinear QPM SHG for duty cycle measurements. The configurations of the non-collinear phase matching scheme are shown in Fig. 1a. The $\vec{k}_{i=1,2}$ vectors represent the wave numbers of the pump and SH and their magnitudes are equal to $2\pi n_i/\lambda_i$, where λ_i are the corresponding wavelengths and n_i are the corresponding refractive indices. \vec{G}_m is the reciprocal lattice vector (RLV) of the crystal. It points in the direction of the poling modulation and its magnitude is $2\pi m/\Lambda$, where Λ is the poling period. The phase matching condition can be written as

$$k_2^2 = 4k_1^2 + G_m^2 - 4k_1 G_m \cos \varphi \quad (1)$$

The ability to non-collinearly phase match the SHG process for different RLV orders can be used to measure the effective average duty cycle of the periodic modulation. The different QPM angles for SHG interaction can be calculated from the non-collinear phase matching condition and are presented in Fig 1b, for all the interactions that were measurable in the experiment (for LiNbO₃ coefficients d_{31} , d_{22} , d_{33} which correspond to *eo*, *oo* and *ee* interactions respectively). The stage rotation angle θ is also the angle between the propagation direction of the fundamental in free-space and the Y axis of the crystal. When θ equals zero, the propagation of the fundamental wave in free-space and inside the crystal is perpendicular to the RLV direction, i.e. $\phi = 90^\circ$. For other values of θ , ϕ is calculated using Snell's law. The efficiency for every interaction is dependent on Fresnel transmissions and reflections, on the walk off between the interacting waves and on the RLV order. Up until now, duty cycle was rarely determined by nonlinear measurements [6], since collinear interaction can be usually phase matched by a single QPM order. We demonstrate here that the average duty cycle can be accurately derived from a set of non-collinear measurements.

The experimental setup is based on a temperature-tuned periodically poled LiNbO₃ (PPLN) optical parametric oscillator source [7], pumped by a 1047 nm Q-switched Nd:YLF, in order to generate signal wavelengths between 1489 and 1537 nm (by varying the 29 μm PPLN crystal

temperature from 100 to 200 °C). The signal wave was adjusted to the desired polarization using a half wave plate followed by a polarizer and then focused to the crystal with a waist radius of $\sim 34 \mu\text{m}$. The SH generator was a $10 \times 7 \times 0.5 \text{ mm}^3$ PPLN crystal with 9 μm period, held in a temperature controlled rotating stage with an angular resolution of 0.016° . The fundamental wave's power was measured by an Ophir 2A-SH thermal detector and the 2ω waves' powers were measured by an Ophir PD-300 silicon detector or by another silicon detector which was amplified and viewed on a scope.

Non-collinear SHG of a 1520 nm pump was used to measure the average duty cycle of the periodically poled crystal, held at 220 °C. While rotating the stage of the crystal to different angles, for phase matching different QPM orders, the SH intensity generated by each RLV as well as the input and output angles were recorded. These angles agree, with better than 1° accuracy, to the calculation (Fig. 1b), and enable to determine the QPM order for each interaction. The measured intensities were compared to a split-step Fourier numerical simulation [7,8], in which the input was a non-depleted single-mode Gaussian beam, having a waist radius of 34 μm in the middle of the crystal. The nonlinear coefficients used for the simulation were $d_{33} = 27 \text{ pm/V}$, $d_{31} = 4.35 \text{ pm/V}$ and $d_{22} = 2.1 \text{ pm/V}$.

The experimental and simulation results are shown in Fig. 2c and d for *eee* and *eo* interactions, respectively, plotted on log scale. The log scale was used since the results span over five-orders of magnitude and cannot be compared on a linear scale. Since zero efficiency of the simulation cannot be plotted on a log scale, it was set to 10^{-9}

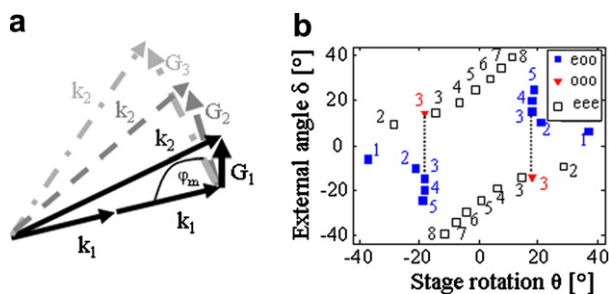


Fig. 1. (a) Vectorial scheme for non-collinear SHG using different RLV's of the same grating. (b) External propagation angle of phase matched SH, δ , with respect to stage rotation angle, θ , for different RLV values and different possible interactions. The dotted lines mark simultaneous generation of cross polarized SH waves.

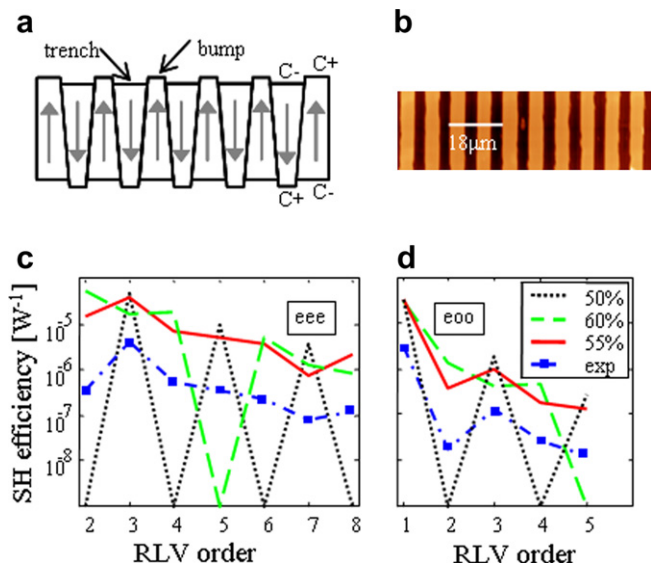


Fig. 2. (a) Periodically poled crystal's domain inversion pattern and topography after etching. (b) Surface scan of the PPLN sample by AFM, (c) *eee* and (d) *eo* SH efficiency with respect to RLV order for different simulated duty cycles, 50% (short dashed black) 60% (long dashed green) and 55% (red line) and experimental results (dashed dot blue). (For interpretation of the references in colour in this figure legend, the reader is referred to the web version of this article.)

W^{-1} for viewing purposes. The comparison between the simulation and experimental efficiency curves indicates clearly that the periodic poling of the crystal has an average duty cycle of 55%. Setting the duty cycle in the simulation to either 50% or 60% results in large changes of the line shapes of the efficiencies, both for *eee* and *ooo* interactions. Hence, the accuracy of this method is better than 5%. The experimental results were measured and shown in Fig. 2c and d to be about one order of magnitude lower than the simulated results. The differences between the measured and calculated efficiencies may be caused by possible deviations of the pump wave from a perfect Gaussian beam, as well as imperfections in the poling process. Since the same crystal and the same pump wave were used for all measured QPM orders, the same deviation from simulation results is expected, thus this constant deviation for all QPM orders should not affect the interpretation of the results in Fig. 2c and d.

In order to characterize the poling period, duty cycle and quality of the poling process it is common to perform surface etching. The surface etching creates trenches in the C– areas, as illustrated in Fig. 2a, which can be scanned locally by atomic force microscope (AFM). AFM scans of both facets of the crystal were taken to validate the duty cycle measurement (a sample scan is shown in Fig. 2b). Ten arbitrary scans of $\sim 90 \times 10 \mu\text{m}^2$ area were taken at each facet and the average duty cycle and period were calculated from all the scans. The original C+ facet had an average duty cycle of $55.4 \pm 1.4\%$ (trench vs. period) and the original C– facet had an average duty cycle of $45.4 \pm 3.9\%$ (bump vs. period), which gives trapezoidal patterns of the inverted domains, as illustrated in Fig. 2a. Since the AFM measurement is done on the crystal surfaces, it can only provide limiting values for the duty cycle that is experienced by the optical wave. The duty cycle inferred by the non-collinear SHG measurement agrees with the range of duty cycles indicated by the surface AFM scans and gives more precise volume estimation. Owing to the local variations in the duty cycle of the sample, the proposed method is sufficiently accurate.

Furthermore, simultaneous generation of two cross polarized non-collinear SH beams was observed, as shown in Fig. 4d. Since this kind of processes is important for quantum optics [2] and all-optical signal processing [3] applications, we have studied it in more detail. The two waves were generated by simultaneous QPM of the non-collinear *ooo* and *ooo* interaction by 3rd-order RLVs of the grating. Further evidence for this simultaneous generation is provided by the calculations shown in Fig. 1b, where the two different processes are simultaneously phase matched for $|\theta| = 18.2^\circ$. This simultaneous generation is not a fortunate coincidence of phase mismatches of the different processes as in collinear interactions [9]. It was shown [7] that non-collinear interactions in one dimensionally poled crystal enable the simultaneous generation of two different processes. This kind of simultaneous generation can be performed in a wide and continuous spectral

range by using the appropriate poling period and incidence angle. The vectorial scheme for the simultaneous cross polarized SHG is shown in Fig. 3b. The pump has an ordinary polarization in the x – y plane and generates simultaneously an ordinary SH wave (using the *ooo* interaction) and an extraordinary SH wave, polarized in the z direction (using the *ooo* interaction). The two different non-collinear phase matching conditions can be solved together to produce the equation for the period of the modulation. The solution is given by

$$\Lambda = 2\pi \left[\frac{m_2 m_1^2 + m_1 m_2^2}{m_2(k_{2e}^2 - 4k_o^2) + m_1(k_{2o}^2 - 4k_o^2)} \right]^{1/2} \quad (2)$$

The solution for the angle ϕ can be achieved by substituting Λ to any of the equations for the non-collinear phase matching conditions. The continuous set of solutions using $m_1 = m_2 = 3$ and temperature of 220°C is presented in Fig. 3a for the spectral range of ~ 1 – $3.5 \mu\text{m}$.

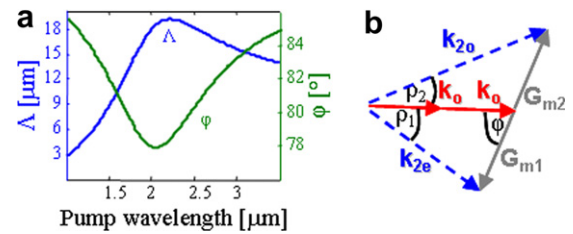


Fig. 3. (a) Period and angle solutions for ~ 1 – $3.5 \mu\text{m}$ pump wavelength for non-collinear cross polarized SHG. (b) Vectorial scheme for non-collinear simultaneous cross polarized SHG.

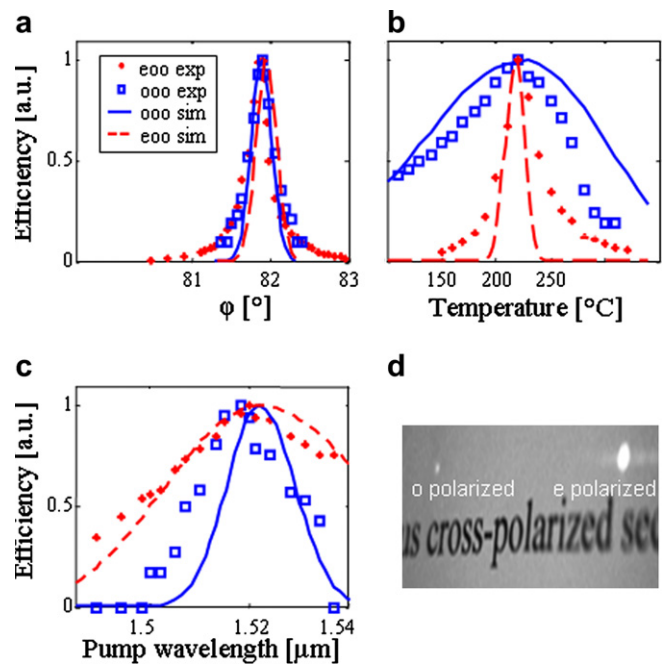


Fig. 4. Angle (a), temperature (b) and wavelength (c) tuning curves for *ooo* interaction (open squares – experimental; solid line – simulation) and *ooo* (diamonds – experimental; dashed line – simulation). (d) Image by Pixelink digital camera of simultaneous cross polarized SHG.

We have measured the angular, thermal and spectral tuning properties of the simultaneous cross polarized SH waves as shown in Fig. 4a,b and c, respectively. The full width at half maximum (FWHM) of the angular tuning was $\sim 0.35^\circ$ for the *ooo* interaction and $\sim 0.3^\circ$ for the *eo* interaction. The thermal FWHM was $\sim 40^\circ\text{C}$ for the *eo* interaction and $\sim 150^\circ\text{C}$ for the *ooo* interaction. The spectral FWHM with respect to the fundamental wavelength was $\sim 60\text{ nm}$ for the *eo* interaction and $\sim 30\text{ nm}$ for the *ooo* interaction. All measured tuning curves fit well with simulated tuning curves results.

We measured the conversion efficiencies for the generated waves using a pump wave of 12 mW average power with pulse width of 8.5 ns and repetition rate of 5.1 kHz. The ordinary and extraordinary SH waves average powers were 9 nW and 235 nW, respectively, corresponding to internal conversion efficiencies of $4.58 \times 10^{-7} \text{ \%W}^{-1}$ and $1.3 \times 10^{-5} \text{ \%W}^{-1}$ (after considering Fresnel transmission of the fundamental and SH waves). The calculated efficiencies are $2.2 \times 10^{-5} \text{ \%W}^{-1}$ for the ordinary SH and $9.3 \cdot 10^{-5} \text{ \%W}^{-1}$ for the extraordinary SH. The differences between efficiencies of the experimental results and the calculations, as was mentioned above, may be caused by possible deviations of the pump wave from a perfect Gaussian beam, as well as imperfections in the poling process. The larger difference for the *ooo* interaction is due to the fact that in LiNbO_3 this interaction generates polarization in the *y* direction which is close to the propagation direction of the SH wave, therefore the efficiency is decreased by a factor of $\sin^2\alpha$ where α is the angle of propagation with respect to the crystal's *y* direction, which gives for $\alpha \sim 15^\circ$ a 15-fold decrease in efficiency.

The wide spectral bandwidth of the simultaneous cross polarized SHG in the non-collinear configuration is useful for frequency doubling of broadband signals, e.g. tunable or ultrashort-pulse sources. Measured bandwidths of the non-collinear SH waves at 760 nm are 7.8 THz and 15.5 THz for the ordinary and extraordinary waves, respectively. The calculated bandwidths for collinear interactions are 234 GHz and 909 GHz for the ordinary and extraordinary waves respectively, which are 33 and 17-fold narrower than the corresponding non-collinear interactions. The non-collinear configuration is also suitable for group velocity matching of one interaction [10] or two interactions [11] simultaneously.

In summary, we have proposed in this article a method to measure the average duty cycle by non-collinear SHG in 1D periodically poled crystal. The derived duty cycle agrees with surface scans of the crystal by AFM. Furthermore, in comparison to our suggested method, the AFM scan has two major downfalls for the assessment of actual duty cycle

which effects the nonlinear interactions. First, it is a surface measurement of the crystal's topography after the etching process, whereas the non-collinear SHG measurement is a volume measurement, in areas which are more relevant for nonlinear interactions, and can thus be used for mapping it inside the crystal. Second, the AFM scan is local ($100 \times 100 \mu\text{m}^2$ is considered a large area to scan), whereas the non-collinear SHG measurement is a macroscopic assessment of the average duty cycle that effects the nonlinear interactions. Moreover, for cases where the structure is not homogeneous and contains widely varying duty cycles the AFM scan can not give the QPM characteristics of the structure whereas the non-collinear measurement averages the inhomogeneity to give the required efficiency predictions. Nonlinear measurement of the average duty cycle can also be performed by collinear QPM [6], but this kind of method requires a tunable source and is not practical for the whole range of poling periods.

Non-collinear interactions also enable simultaneous SHG of cross polarized light. The conversion efficiency dependence on the crystal temperature, entrance angle and pump wavelength was measured, and agrees well with numerical simulations. Spectral widths of the non-collinear interaction were found to be significantly larger than those of collinear interactions and may be used for simultaneous generation of cross polarized light from broadband sources.

Acknowledgements

This work was supported by the Israel Science Foundation, Grant No. 960/05 and by the Israeli Ministry of Science. We thank S.M. Saltiel for fruitful discussions.

References

- [1] M.M. Fejer, G.A. Magel, D.H. Jundt, R.L. Byer, IEEE J. Quantum Elect. 28 (1992) 2631.
- [2] R.C. Pooser, O. Pfister, Opt. Lett. 30 (2005) 2635.
- [3] S. Saltiel, Y. Deyanova, Opt. Lett. 24 (1999) 1296.
- [4] J.U. Kang, Y.J. Ding, W.K. Burns, J.S. Melinger, Opt. Lett. 22 (1997) 862.
- [5] E. Rabia, A. Arie, Appl. Opt. 45 (2006) 540.
- [6] X.P. Zhang, J. Hebling, J. Kuhl, W.W. Rhle, H. Giessen, Opt. Lett. 26 (2001) 2005.
- [7] T. Ellenbogen, A. Arie, S.M. Saltiel, Opt. Lett. 32 (2007) 262.
- [8] G.P. Agrawal, Nonlinear Fiber Optics, Academic, Boston Mass., 1995.
- [9] V. Pasiskevicius, S.J. Holmgren, S. Wang, F. Laurell, Opt. Lett. 27 (2002) 1628.
- [10] S. Ashihara, T. Shimura, K. Kuroda, J. Opt. Soc. Am. B 20 (2003) 853.
- [11] S.M. Saltiel, Y.S. Kivshar, Opt. Lett. 31 (2006) 3321.